Available online at www.sciencedirect.com
ScienceDirect
Journal of Molecular Catalysis A: Chemical 270 (2007) 185–194
JOURNAL OF MOLECULAR CATALYSIS A: CHEMICAL
www.elsevier.com/locate/molcata

Synthesis and catalytic properties in olefin epoxidation of dioxomolybdenum(VI) complexes bearing a bidentate or tetradentate *salen*-type ligand

Sofia M. Bruno [a], Salete S. Balula [a], Anabela A. Valente [a], Filipe A. Almeida Paz [a], Martyn Pillinger [a], Carla Sousa [b,1], Jacek Klinowski [c], Cristina Freire [b], Paulo Ribeiro-Claro [a], Isabel S. Gonçalves [a,*]

[a] *Department of Chemistry, CICECO, University of Aveiro, Campus de Santiago, 3810-193 Aveiro, Portugal*
[b] *REQUIMTE, Departamento de Química, Faculdade de Ciências, Universidade do Porto, 4169-007 Porto, Portugal*
[c] *Department of Chemistry, University of Cambridge, Lensfield Road, CB2 1EW Cambridge, United Kingdom*

Received 24 November 2006; received in revised form 25 January 2007; accepted 31 January 2007
Available online 6 February 2007

Abstract

The monomeric *cis*-dioxomolybdenum(VI) complexes [MoO_2(oep-saldpen)] and [MoO_2Cl_2(oep-H_2saldpen)], with a tetradentate [N_2(imine)O_2] and bidentate [N_2(imine)] *salen*-type ligand functionalised with two pyrrole derivative pendant arms [oep-H_2saldpen = 1,2-diphenylethylenebis(3-oxyethylpyrrole)salicylideneimine], were synthesised and characterised by ^{1}H NMR, IR and Raman spectroscopy. The solid-state structure of the free ligand oep-H_2saldpen was determined by single crystal X-ray diffraction. Assignment of the vibrational spectra of the molybdenum complexes was supported by carrying out ab initio calculations for the possible isomers using [MoO_2(salen)] and [MoO_2Cl_2(H_2salen)] as model compounds [H_2salen = *N*,*N*′-ethylenebis(salicylideneimine)]. The oep-saldpen complexes were examined as catalysts for the epoxidation of cyclooctene, (*R*)-(+)-limonene, styrene, α-pinene, and *cis* and *trans*-β-methylstyrene, with *tert*-butyl hydroperoxide as the oxidant. Both complexes exhibited high selectivity for the epoxidation reaction, with the bis(chloro) complex being always the more active of the two.

Keywords: Molybdenum; Oxide complexes; *Salen*-type ligands; Pyrrole derivatives; Epoxidation

1. Introduction

Epoxides are important organic intermediates since they undergo ring-opening reactions with a variety of reagents to give mono- or bi-functional organic products [1,2]. One of the preferred methods of epoxide synthesis is the reaction of olefins with hydrogen peroxide or alkyl hydroperoxides, catalysed by transition metal complexes [3,4]. Molybdenum catalysts are very versatile in olefin epoxidation and are the basis of important industrial processes for the epoxidation of propylene, with alkyl hydroperoxides as the oxygen source [3,5–7]. There has been continuing effort to prepare new complexes with tailored catalytic properties [8–22] and to elucidate the reaction mechanisms [4,23–31]. A large number of oxomolybdenum(VI) complexes with the *cis*-MoO_2 fragment have been studied, and include compounds of the type [$MoO_2X_2(L^1)_n$], [$MoO_2X(L^2)_m(L^1)_n$] and [$MoO_2(L^2)_m(L^1)_n$] (X = Cl, Br, CH_3, OR etc; L = neutral (L^1) or anionic (L^2) N,O,S-ligand). These complexes are usually six-coordinate, exhibiting a distorted octahedral coordination geometry. Complexes with the general formula [MoO_2L] containing tetradentate *salen* ligands are a potentially interesting subset of this family [32–39], especially since the structures of *salen* ligands are easily tuned, both sterically and electronically, by the appropriate choice of the salicylaldehyde derivative and the diamine components. Although the first dioxomolybdenum(VI) complexes bearing *salen*-type ligands were prepared and spectroscopically characterised as long ago as 1974 [32], their catalytic application for

* Corresponding author. Fax: +351234370084.
E-mail address: igoncalves@dq.ua.pt (I.S. Gonçalves).
[1] Present address: Faculdade de Ciências da Saúde, Universidade Fernando Pessoa, Rua Carlos da Maia no. 296, 4200-150 Porto, Portugal

1381-1169/$ – see front matter © 2007 Elsevier B.V. All rights reserved.
doi:10.1016/j.molcata.2007.01.050

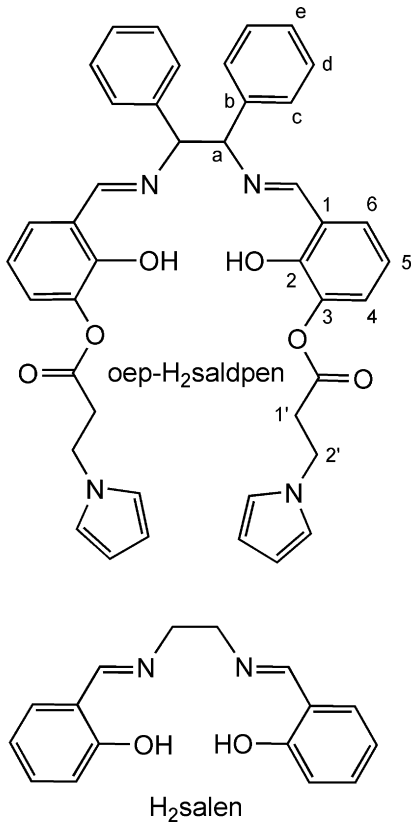

Plate 1.

epoxidation reactions has only recently been explored [38,39]. Here we describe the synthesis, characterisation and catalytic performance in olefin epoxidation of dioxomolybdenum(VI) complexes containing a *salen*-type ligand functionalised with two pyrrole derivative pendant arms. The structure of the free ligand was determined by single crystal X-ray diffraction. It has two mixed N,O-type coordination sites: one that comprises the N_2(imine)O_2 donor atoms, which are well suited for the coordination of transition metal cations, and the other composed of the coordinating atoms within the pyrrole derivative pendant arms (Plate 1).

2. Experimental

2.1. Materials and methods

Microanalyses for CHN were performed at the University of Aveiro. IR spectra were obtained as KBr pellets using a FTIR Mattson-7000 infrared spectrophotometer. Raman spectra were recorded on a Bruker RFS100/S FT instrument (Nd:YAG laser, 1064 nm excitation, InGaAs detector). ^{1}H NMR spectra were acquired using a Bruker CXP 300 spectrometer. Solid-state magic-angle-spinning (MAS) NMR spectra were recorded at 100.62 MHz on a Bruker Avance 400 spectrometer. ^{13}C CP MAS NMR spectra were recorded with 3.5 μs ^{1}H 90° pulses and 2 ms contact time, with a spinning rate of 7 kHz and 4 s recycle delays. Chemical shifts are quoted in parts per million from tetramethylsilane.

All preparations and manipulations were carried out using standard Schlenk techniques under nitrogen. Solvents were dried by standard procedures (*n*-hexane, diethyl ether and THF with Na/benzophenone ketyl; dichloromethane and 1,2-dichloroethane with CaH_2), distilled under nitrogen and kept over 4 Å molecular sieves. 1,2-Diphenylethylenebis(3-oxyethylpyrrole)salicylideneimine (oep-H_2saldpen, Plate 1) was prepared as described previously [40]. $MoO_2(acac)_2$ and MoO_2Cl_2 were purchased from Aldrich and used as received.

2.2. *[MoO_2[1,2-diphenylethylenebis(3-oxyethylpyrrole)salicylideneiminate]] (**1**)*

A solution of oep-H_2saldpen (0.59 g, 0.85 mmol) in CH_2Cl_2 (30 mL) was stirred for 15 min. $MoO_2(acac)_2$ (0.28 g, 0.86 mmol) was then added and the mixture stirred for 16 h. The solution was evaporated to dryness and the resultant orange solid washed with diethyl ether and dried under vacuum, giving an overall yield of 0.66 g (94%) of **1**. Anal. found: C, 61.73; H, 4.93; N, 7.24. $C_{42}H_{36}N_4MoO_8$ (820.70) requires C, 61.47; H, 4.42; N, 6.83. IR (KBr, cm^{-1}): 3139m, 3100m, 3057m, 3028m, 2927m, 2888m, 1752s, 1628vs, 1597m, 1547m, 1500s, 1462s, 1423m, 1366m, 1342w, 1285s, 1260s, 1234s, 1220s, 1202s, 1149vs, 1093m, 1073 s, 1033m, 985w, 941m, 928m, 907s, 877m, 855m, 825w, 786w, 769s, 750s, 727vs, 703s, 607m, 578w, 552w, 531m, 508w, 435m. Raman (cm^{-1}): 3139w, 3125w, 3111w, 3103w, 3058s, 2981m, 2937m, 2927m, 1630vs, 1599m, 1587m, 1547w, 1500w, 1463s, 1447w, 1424w, 1386s, 1311m, 1286m, 1235s, 1197w, 1163w, 1096w, 1074w, 1061m, 1028w, 1001s, 948m, 905vw, 874m, 851w, 823w, 617w, 607w, 573w, 535w, 492w, 392m, 343w, 326w, 301w, 249m, 204w, 175w. ^{1}H NMR (300 MHz, $(CD_3)_2CO$, 25 °C): δ = 8.46 (s, 2H, N=CH), 7.52-7.05 (m, 16H, C4,5,6,c,d,e-H), 6.87–6.81 (m, 4H, αα′-pyrrole), 6.06 (m, 4H, ββ′-pyrrole), 5.13 (s, 2H, Ca-H), 4.38-4.33 (t, 4H, C2′H_2), 3.11-3.07 (t, 4H, C1′H_2) ppm.

2.3. *[MoO_2Cl_2[1,2-diphenylethylenebis(3-oxyethylpyrrole)salicylideneimine]] (**2**)*

The solvent adduct [$MoO_2Cl_2(THF)_2$] was prepared by dissolving MoO_2Cl_2 (0.11 g, 0.54 mmol) in THF (10 mL) at 50 °C and evaporating the solution to dryness. A solution of oep-H_2saldpen (0.30 g, 0.43 mmol) in CH_2Cl_2 (20 mL) was then added to a solution of [$MoO_2Cl_2(THF)_2$] in CH_2Cl_2 (20 mL) and the reaction mixture left to stir at room temperature for 4 h. The solution was filtered, evaporated to dryness and the resultant yellow solid washed with diethyl ether and dried under vacuum, giving an overall yield of 0.39 g (95%) of **2**. Anal. found: C, 56.65; H, 4.04; N, 6.96. $C_{42}H_{38}N_4Cl_2MoO_8$ (893.62) requires C, 56.45; H, 4.29; N, 6.27. IR (KBr, cm^{-1}): 3100m, 3057m, 3028m, 2927m, 2887m, 1752s, 1630vs, 1606w, 1560m, 1498s, 1482s, 1458s, 1420m, 1391m, 1365w, 1284s, 1269vw, 1233vs, 1201s, 1149vs, 1086s, 1073s, 1031m, 967s, 943w, 919s, 907m, 862m, 825w, 798w, 759m, 749m, 728vs, 704vs, 610m, 566w, 552w, 530w, 509w, 440w, 336m. ^{1}H NMR (300 MHz, $(CD_3)_2CO$, 25 °C): δ = 10.09 (s, 2H, OH), 8.50 (s, 2H, N=CH),

7.53-7.07 (m, 16H, C4,5,6,c,d,e-H), 6.88-6.83 (m, 4H, αα′-pyrrole), 6.05-6.02 (m, 4H, ββ′-pyrrole), 5.19 (s, 2H, Ca-H), 4.38-4.33 (t, 4H, C2′H_2), 3.15-3.10 (t, 4H, C1′H_2) ppm.

2.4. Single crystal X-ray diffraction

Yellow crystals of oep-H_2saldpen were prepared by slow diffusion of diethyl ether into a solution of the ligand in CH_2Cl_2. A suitable single-crystal was mounted on a glass fibre using FOMBLIN Y perfluoropolyether vacuum oil (LVAC 25/6) purchased from Aldrich [41]. Data were collected at 180(2) K on a Nonius Kappa charge-coupled device area-detector diffractometer (Mo Kα graphite-monochromated radiation, λ = 0.7107 Å), equipped with an Oxford Cryosystems cryostream and controlled by the Collect software package [42]. Images were processed using the software packages Denzo and Scalepack [43], and data corrected for absorption by the empirical method employed in Sortav [44,45]. The structure was solved using the direct methods implemented in SHELXS-97 [46] and refined by full-matrix least squares on F^2 using SHELXL-97 [47]. All non-hydrogen atoms were successfully located from difference Fourier maps and refined using anisotropic displacement parameters.

Hydrogen atoms attached to carbon were located at their idealised positions using appropriate *HFIX* instructions in SHELXL (43 for the aromatic groups and 13 or 23 for the –CH tertiary or –CH_2 secondary carbon atoms, respectively) and included in subsequent refinement cycles in riding-motion approximation with isotropic thermal displacement parameters (U_{iso}) fixed at 1.2 times U_{eq} for the carbon atom to which they were attached. The hydrogen atom [H(1A)] belonging to the crystallographically independent hydroxyl group of oep-H_2saldpen was markedly visible as a *Q* peak in the last difference Fourier map calculated from successive least-squares refinements. However, this atom was included in the final crystal structure model by employing the *AFIX* 147 instruction in SHELXL in riding-motion approximation with U_{iso} fixed at $1.5 \times U_{eq}$[O(1)]. This procedure envisages the optimisation of the intramolecular hydrogen bonding interaction between the hydroxyl group and the neighbouring nitrogen acceptor atom.

The last difference Fourier map synthesis showed the highest peak (0.567 eÅ^{-3}) and deepest hole (−0.646 eÅ^{-3}) located at 1.01 Å from C(7) and 1.87 Å from C(9), respectively. Information concerning crystallographic data collection and structure refinement details is summarised in Table 1. Bond lengths and angles involving non-hydrogen atoms of the asymmetric unit are provided in Tables S1 and S2 in the Electronic Supplementary Material.

Crystallographic data (excluding structure factors) for the crystal structure of oep-H_2saldpen have been deposited with the Cambridge Crystallographic Data Centre as supplementary publication no. CCDC-628098. These data can be obtained free of charge at http://www.ccdc.cam.ac.uk/conts/retrieving.html [or from the Cambridge Crystallographic Data Centre, 12 Union Road, Cambridge CB2 2EZ, U.K. Fax: (international) +44 1223 336 033; e-mail: deposit@ccdc.cam.ac.uk].

Table 1
Crystal and structure refinement data for oep-H_2salpden

Formula	$C_{42}H_{38}N_4O_6$
Formula weight	694.76
Crystal system	Triclinic
Space group	$P\bar{1}$
a (Å)	9.6894(2)
b (Å)	9.9975(2)
c (Å)	10.5557(3)
α (°)	81.5388(11)
β (°)	76.9289(11)
γ (°)	63.8804(9)
Volume (Å^3)	892.99(4)
Z	1
D_c (g cm^{-3})	1.292
μ(Mo-Kα) (mm^{-1})	0.087
F(0 0 0)	366
Crystal size (mm)	0.42 × 0.30 × 0.28
Crystal type	Colourless blocks
θ range	3.52–27.50
Index ranges	$-12 \le h \le 12$, $-12 \le k \le 12$, $-13 \le l \le 13$
Reflections collected	10447
Independent reflections	4075 (R_{int} = 0.0305)
Final R indices [I > 2σ(I)][a,b]	$R1$ = 0.0616, $wR2$ = 0.1564
Final R indices (all data)[a,b]	$R1$ = 0.0751, $wR2$ = 0.1689
Weighting scheme[c]	m = 0.0905, n = 0.2458
Largest diff. peak and hole	0.567 and −0.646 eÅ^{-3}

[a] $R1 = \sum ||F_o| - |F_c|| / \sum |F_o|$.

[b] $wR2 = \sqrt{\sum \left[w(F_o^2 - F_c^2)^2\right] / \sum \left[w(F_o^2)^2\right]}$.

[c] $w = 1/[\sigma^2(F_o^2) + (mP)^2 + nP]$ where $P = (F_o^2 + 2F_c^2)/3$.

2.5. Ab initio calculations

Ab initio calculations were performed using the G03w program package [48], running on a personal computer. The fully optimised geometry, the harmonic vibrational frequencies, and the infrared and Raman intensities were obtained at the B3LYP level, using the valence double-zeta basis set of Dunning and Hay [49] (Lanl2DZ basis set of G03). Due to the large size of the systems, the ligand oep-H_2saldpen was replaced by the model ligand *N*,*N*′-ethylenebis(salicylideneimine) (H_2salen, Plate 1), giving model complexes hereafter referred to as [MoO_2(salen)] and [MoO_2Cl_2(H_2salen)]. The calculated wavenumbers were scaled by a factor of 0.961 before comparison with the experimental values [50].

2.6. Catalysis

The liquid-phase catalytic epoxidations were carried out at atmospheric pressure in a reaction vessel equipped with a magnetic stirrer and immersed in a thermostated oil bath. A 1% molar ratio of complex/substrate and a substrate/oxidant molar ratio of 0.63 were used. *tert*-Butyl hydroperoxide was used as the oxygen donor (5.5 M in decane) and different substrates were studied, namely cyclooctene, (*R*)-(+)-limonene, styrene and α-pinene. The reactions were carried out without additional solvent (other than the decane present in the *t*-BuOOH solution) or using *n*-hexane or 1,2-dichloroethane as co-solvent (2 mL solvent for 1.7 mmol substrate). The course of the reac-

tion was monitored using a gas chromatograph (Varian 3800) equipped with a capillary column (DB-5, 30 m × 0.25 mm) and a flame ionisation detector. Products were identified by gas chromatography–mass spectrometry (HP 5890 Series II GC; HP 5970 Series Mass Selective Detector) using He as carrier gas. The catalytic properties for the asymmetric epoxidation of pro-chiral olefins were investigated and these experiments were monitored using a Varian 3900 GC equipped with a CyclosilB 30 m × 0.25 mm column.

3. Results and discussion

3.1. Crystal structure of oep-H_2saldpen

The *salen*-type ligand oep-H_2saldpen with two OC(O) $CH_2CH_2NC_4H_4$ pendant arms was prepared in a multi-step procedure as described previously [40]. The molecule crystallised (from CH_2Cl_2/Et_2O) in the centrosymmetric triclinic space group $P\bar{1}$, with the asymmetric unit comprising only half of the molecular unit (Fig. 1) and, remarkably, no solvent molecules. The crystallographic evidence is in good agreement with the symmetry of the individual molecule, which is formed by two identical fragments joined together by a C–C bond between the two tertiary carbon atoms.

In the crystal structure of oep-H_2saldpen, the majority of the internal bonds of the molecular unit, which are chemically capable of internal conformational rotations, are actually distributed in a way that significantly minimises the steric hindrance imposed by the close proximity of several large functional groups. This is particularly evident for the central C(7)–C(7)^i bond [1.537(4) Å; symmetry code: (*i*) 2-*x*, 1-*y*, 1-*z*] which appears rotated such that each of the large substituents is located, within the molecular unit, as far as spatially possible from its symmetry-generated identical fragment. Indeed, as represented in Fig. 1, the two benzyl groups and the two 3-substituted salicylidene residues are placed in two planes intersecting at the inversion centre located in the middle of the aforementioned C(7)–C(7)^i bond. The dihedral angle between these two planes is about 70.8° and is geometrically imposed solely by the rigid tetrahedral environment of the C(7) atom. The rotation around the C(7)–C(7)^i bond is also largely facilitated by the intramolecular hydrogen bond interaction within the neighbouring 3-substituted salicylidene residues. This was also registered for *N*,*N*′-ethylenebis(salicylideneimine), as reported by Pahor et al. [51]. Indeed, the spatial proximity between the hydroxyl group and the nitrogen atom leads to the formation of an energetically favourable internal O–H···N hydrogen bonding interaction ($d_{O\ldots N}$ 2.5787(18) Å and ∠(OHN) 146°), thus creating an extra five-membered ring (Fig. 1) best described by the graph set motif *S*(*6*) [52]. This reduces conformational flexibility and creates additional steric hindrance for this moiety.

The spatial arrangement of the external pyrrole-CH_2–CH_2–CO_2– moiety in the crystal structure of oep-H_2saldpen reflects, as expected, the various degrees of conformational flexibility arising from the presence of the two –CH_2 secondary groups. However, the structural arrangement of this group is also largely driven by the existence of intermolecular interactions with other molecular units, namely weak, but highly directional C–H···π contacts between a C–H bond of the pyrrole group and the 3-substituted salicylidene aromatic ring of a neighbouring oep-H_2saldpen ($d_{C\ldots Cg}$ 3.390(1) Å with ∠(CHC_g) ca. 156° – see Fig. 2; C_g stands for the centroid of the 3-substituted salicylidene aromatic ring). Interactions between adjacent oep-H_2saldpen moieties are further assured by π–π contacts between neighbouring 3-substituted salicylidene aromatic rings which are in close proximity due to crystal packing (not shown), which is also mediated by the need to effectively fill the void space via van der Waals interactions. Remarkably, the crystal structure of *N*,*N*′-ethylenebis(salicylideneimine) does not show any evidence for the presence of such weak C–H···π or π–π intermolecular interactions.

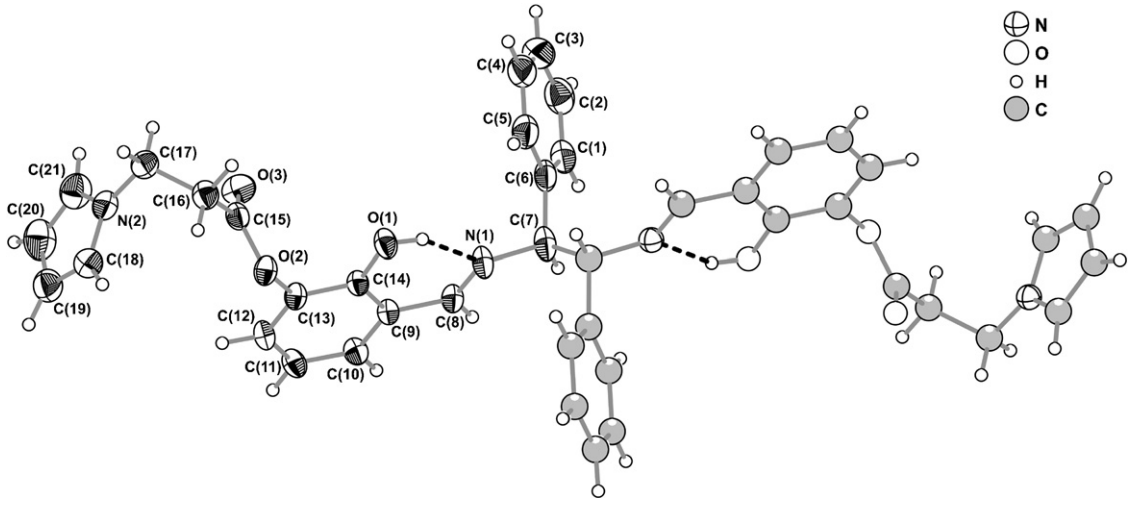

Fig. 1. Schematic representation of the molecular unit of oep-H_2saldpen. Atoms belonging to the asymmetric unit are represented with thermal ellipsoids drawn at the 50% probability level. The intramolecular O–H···N hydrogen bonding interactions [with $d_{O\ldots N}$ 2.5787(18) Å and ∠(OHN) 146°] are represented as dashed lines. Selected bond lengths and angles are given in Tables S1 and S2 in the Electronic Supplementary Material.

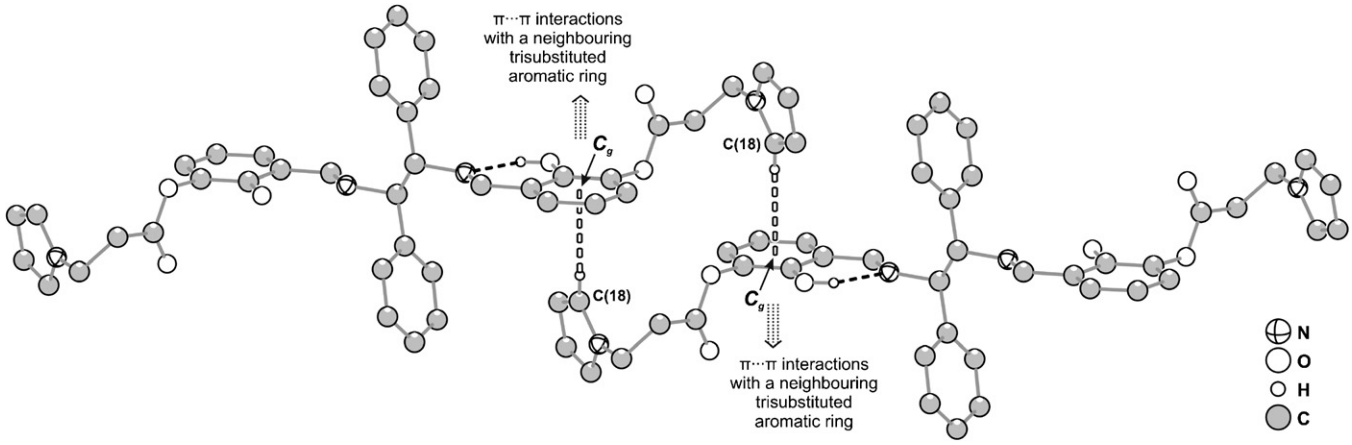

Fig. 2. Schematic representation of the highly directional C—H···π contacts (white-filled dashed lines) connecting neighbouring molecules of oep-H_2saldpen: $d_{C\ldots Cg}$ 3.390(1) Å and ∠(CHC_g) ca. 156° (where C_g stands for the centroid of the 3-substituted salicylidene aromatic ring of oep-H_2saldpen). Hydrogen atoms which are not involved in either hydrogen bonding interactions (black-filled dashed lines) or C—H···π contacts, and symmetry transformations used to generate equivalent atoms, have been omitted for clarity.

3.2. Synthesis and characterisation of the dioxomolybdenum(VI) complexes

Reaction of $[MoO_2(acac)_2]$ or $[MoO_2Cl_2(THF)_2]$ with 1 eq. of oep-H_2saldpen in CH_2Cl_2 gave the complexes $[MoO_2$(oep-saldpen)] (**1**) and $[MoO_2Cl_2$(oep-H_2saldpen)] (**2**), respectively. Assuming that both compounds are monomeric and six-coordinate, the molecular formulae indicate that the coordination mode of the ligand is tetradentate $[N_2(imine)O_2]$ in **1** and bidentate $[N_2(imine)]$ in **2** (Plate 2). These coordination modes were confirmed and further investigated using ^{1}H-NMR, IR and Raman spectroscopy.

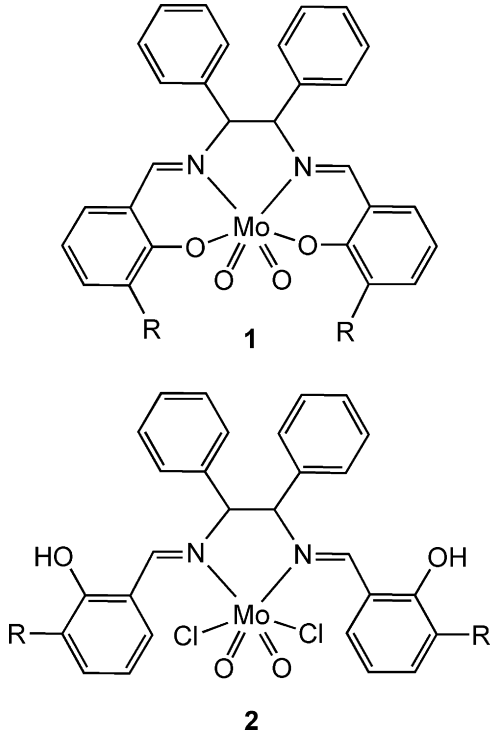

Plate 2.

The ^{1}H NMR spectrum of the free ligand oep-H_2saldpen shows a resonance at about 13.5 ppm for the aromatic OH group. Disappearance of this signal after reaction with $[MoO_2(acac)_2]$ indicates a coordination of the phenolic oxygen to the metal in compound **1**. A signal at 10.1 ppm for compound **2** is attributed to unbound aryl-OH groups. Coordination of both nitrogen atoms of the organic ligand to the metal centre in compounds **1** and **2** is indicated by a shift of the signal for the imine carbon protons from 8.1 ppm for the free ligand to about 8.5 ppm for the complexes. Similar shifts were reported previously for other dioxomolybdenum(VI) complexes bearing tridentate or tetradentate Schiff base ligands derived from salicylaldehyde [38,53,54]. The presence of only one azomethine resonance for **1** and **2** is consistent with the presence of only the α-*cis* isomer in solution (Plate 3). This is because the α-*cis* isomer possesses a two-fold axis which bisects the N–CHR–CHR–N chain, and therefore the two CH=N protons are expected to be equivalent [33,34]. The β-*cis* isomer is less symmetrical and compounds with this structure usually give at least two signals in the ^{1}H-NMR spectrum. Like complex **1**, the compound $[MoO_2$(saldpen)] was reported to show only one resonance for

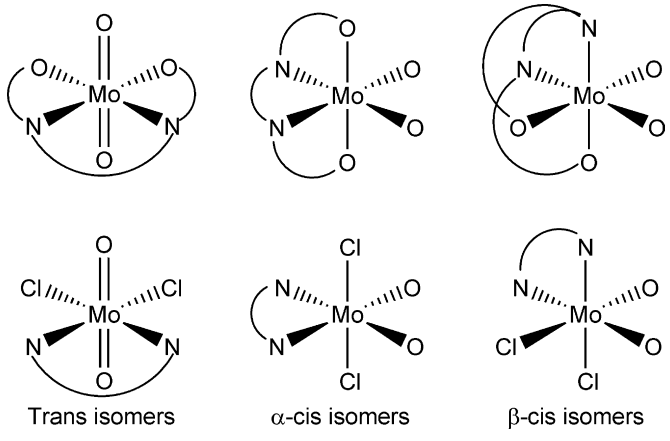

Plate 3.

the azomethine group and therefore its structure in solution was proposed to be α-*cis* [34].

The IR spectrum of the free ligand oep-H_2saldpen in the solid state exhibits a weak broad ν(OH) absorption in the region 2600–2800 cm^{-1} assignable to the intramolecularly hydrogen-bonded OH group. This band disappears in the spectra of the complexes, consistent with a change in the conformation of the ligand and (in the case of complex **1**) deprotonation of the OH group and the formation of the Mo–O bonds. The assignment of the vibrational spectra was assisted by carrying out ab initio calculations for the *trans*, α-*cis* and β-*cis* isomers using [MoO_2(salen)] and [MoO_2Cl_2(H_2salen)] as model complexes (Plate 3 and Table 2). Complexes **1** and **2** exhibit the C=O (pendant arm) and C=N(imine) bond stretching vibrations as strong bands in the IR spectra at 1752 and 1628 cm^{-1}, respectively, and these are unshifted relative to the positions of the corresponding bands in the free ligand. On the other hand, the lower wavenumber component of the new ν(C=N) mode at 1586 cm^{-1} for the free ligand is replaced by bands at 1597 cm^{-1} for **1** and 1606 cm^{-1} for **2**. The IR spectra of the complexes also exhibit two strong ν(Mo=O) bands at 907 and 941 cm^{-1} for **1**, and 919 and 967 cm^{-1} for **2**, characteristic of the asymmetric and symmetric stretching vibrations of the *cis*-$[MoO_2]^{2+}$ fragment [30]. The comparatively higher ν(Mo=O) frequencies observed for **2** indicate that the Mo=O bonds are strengthened when the Mo–O(phenolate) bonds are replaced by Mo–Cl bonds. Similar trends were also found for chloro and triphenylsiloxy derivatives of the type [MoO_2X_2L] (X = Cl or $OSiPh_3$) chelated with bidentate pyrazolylpyridine ligands (L) [55]. The ν(Mo–N), ν(Mo–O) (phenolate) and ν(Mo–Cl) vibrations for complexes **1** and **2** appear below 650 cm^{-1}. In the Raman spectrum of **1** (a good quality spectrum for **2** could not be obtained), a weak band at 326 cm^{-1} is assigned to ν(Mo–N) and lies within the reported range of 310–340 cm^{-1} for dioxomolybdenum(VI) complexes bearing sugar-derived chiral Schiff-base ligands of general formula [MoO_2(L)(Solv)] [12]. A band at 607 cm^{-1} is assigned to the ν(Mo–O) vibration coming from the molybdenum-bound phenolic oxygen. For complex **2**, a band at 336 cm^{-1} in the IR spectrum is assigned as the ν(Mo–Cl) vibration.

A comparison of the calculated Mo=O, Mo–N and Mo–O or Mo–Cl stretching frequencies with the experimental values allows us to infer which type of isomer is likely to be dominant in the solid state. It was shown by ^{1}H-NMR that the complex [MoO_2(salen)] has a β-*cis* configuration in solution [32–34]. In the solid-state, the ν(Mo=O) vibrations are found at 885 and 915 cm^{-1} [34], in very good agreement with the calculated values for the β-*cis* isomer (Table 2). The β-*cis* configuration also seems to be the dominant species in the solid state for complex **1**, while for complex **2** there is a better match between the experimental and calculated wavenumbers for the α-*cis* isomer [56]. As described above, the ^{1}H NMR data for **1** and **2** suggest that the α-*cis* structures are the main isomers present in solution. If the solid-state configuration for **1** is β-*cis*, this indicates that isomerisation occurs in solution. Isomerisation has been characterised previously for complexes of the type [MoO_2L] containing tetradentate *salen*-type ligands by comparing solution ^{1}H NMR data with the solid-state structures determined by single crystal X-ray diffraction [34]. Attempts to prepare suitable crystals of **1** have so far been unsuccessful and therefore an isomerisation process in solution is yet to be confirmed.

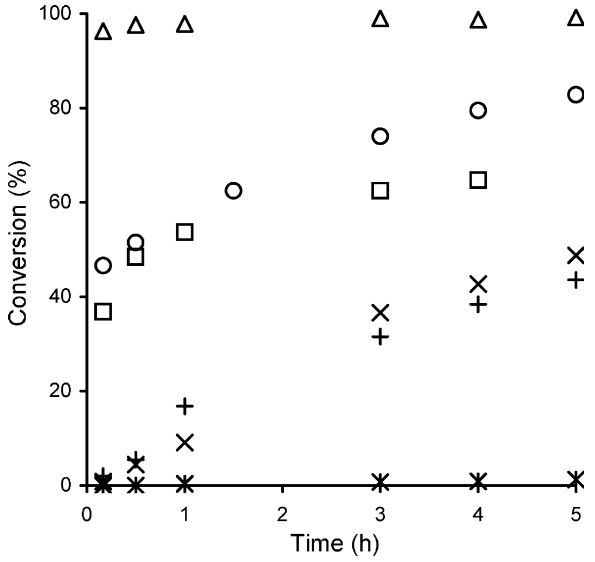

Fig. 3. Kinetics of the epoxidation of cyclooctene with *t*-BuOOH (in decane), using different co-solvents, at 55 °C in the presence of **1** (DCE ×, *n*-hexane *, none +) or **2** (DCE Δ, *n*-hexane □, none ◯).

3.3. Catalysis

Compounds **1** and **2** were tested as catalysts for olefin epoxidation using cyclooctene as a model substrate and *tert*-butyl hydroperoxide (*t*-BuOOH in decane) as oxygen donor, without co-solvent, at 55 °C. Control experiments showed that practically no epoxide was formed without catalyst or with the pure Schiff base ligand oep-H_2saldpen. In the presence of the Mo^{VI} complexes, 1,2-epoxycyclooctane was obtained as the only product with yields after 24 h of 75% for **1** and 98% for **2**. These results indicate that the active species contain molybdenum. The kinetic profile of **2** is typical of dioxomolybdenum(VI) complexes belonging to the [MoO_2Cl_2L] family, tested as catalysts under similar reaction conditions (Fig. 3). After an initially abrupt increase in cyclooctene conversion, the reaction slows down considerably with the course of time. Previous investigations revealed that, in a first elementary step, *t*-BuOOH coordinates to the Mo centre and a proton is transferred from *t*-BuOOH to one of the Mo=O groups of the complex, leading to the formation of an intermediate Mo^{VI} alkylperoxo complex [26]. An oxygen atom is then transferred from the Mo-bound peroxo to the olefin, resulting in the formation of the epoxide and *tert*-butanol. The latter is a by-product that competes with *t*-BuOOH for coordination to the metal centre, gradually retarding the overall reaction [26,30].

The epoxidation reaction is much faster in the presence of **2** than of **1** (Fig. 3), with initial catalytic activities of 280 and 12 mol mol_{Mo}^{-1} h^{-1}, respectively (Table 3). The different activities are probably a consequence of the complex interplay of steric and electronic factors. Differences in solubility are unlikely to be relevant since the solubility of **1** and **2** in

Table 2
Selected IR and Raman stretching frequencies of complexes **1** and **2** and calculated (B3LYP) frequencies for the three possible isomers of the model complexes $[MoO_2(salen)]$ and $[MoO_2Cl_2(H_2salen)]$

Complex	Calcd[a] for the isomers			IR (cm^{-1})[b]	Raman (cm^{-1})	Tentative assignment
	trans	α-*cis*	β-*cis*			
1	392, 422	427, 428	378, 489	–	326w	ν(Mo—N)
	628	577, 588	519, 625	607m	607w	ν(Mo—O)
	803, 820	911, 912	881, 917	907s, 941m	905vw, 948m	ν(Mo=O)
	1614, 1617	1575, 1579	1567, 1610	1597m, 1628vs	1599m, 1630vs	ν(C=N)
2	335, 355	270[c],313	338	336m	–	ν(Mo—Cl)
	493, 497	270[c], 388	218	–	–	ν (Mo—N)
	833, 853	915, 925	893, 922	919s, 967s	–	ν(Mo=O)
	1645	1602, 1625	1616, 1639	1606w, 1630vs	–	ν(C=N)

[a] Scaled values above 500 cm^{-1} (scale factor = 0.961).
[b] *Abbreviations*: vs = very strong, vw = very weak, s = strong, m = medium, w = weak.
[c] Highly mixed stretching vibrations.

the reaction medium is quite poor and apparently similar for both catalysts. The Lewis acidity of dioxomolybdenum(VI) complexes is one of the most important characteristics that determines catalytic performance in olefin epoxidation [26,57]. The major role of the Mo^{VI} centre is to withdraw electrons from the peroxidic oxygen making it more susceptible to be attacked by nucleophiles such as olefins. High turnover frequencies (TOFs) are often associated with a low electron density at the metal centre [26]. We may assume that an increase in the Lewis acidity at the metal centre will increase the molybdenum–oxygen bond order [26,58,59]. Hence, the higher ν(Mo=O) wavenumbers observed for **2** against **1** are consistent with a higher Lewis acidity at the metal centre for the bis(chloro) complex [58,59]. Assuming that the reaction mechanism is the same for both compounds, the coordination of *t*-BuOOH to the metal centre to form the active oxidising species should therefore be more favourable for complex **2**, which would contribute to a higher initial reaction rate. We may also expect that steric hindrance in **1** resulting from the presence of the coordinated phenoxide groups will have a detrimental effect on catalytic activity.

Table 3
Catalytic performance of **1** and **2** in the epoxidation of olefins with *t*-BuOOH

Cat.	Substrate	Solvent	TOF[a] (mol mol_{Mo}^{-1} h^{-1})	Conv.[b] (%)	Select.[c] (%)
1	Cyclooctene	None (run 1)	12	75	100
		None (run 2)[d]	8	57	100
		None[e]	9	41	100
		Dichloroethane	5	81	100
		n-hexane	<1	12	100
	(*R*)-(+)-Limonene	Dichloroethane	–	50	100
	α-Pinene	Dichloroethane	–	9	24[f]
	Styrene	Dichloroethane	–	2	100
	trans-β-Methylstyrene[g]	Dichloromethane	<1	5	1 (ee)[h]
	cis-β-Methylstyrene[g]	Dichloromethane	3	6	8 (ee)[h]
2	Cyclooctene	None (run 1)	280	98	100
		None (run 2)[d]	33	88	100
		None[e]	59	71	100
		Dichloroethane	578	100	100
		n-hexane	221	81	100
	(*R*)-(+)-Limonene	Dichloroethane	–	65	100
	α-Pinene	Dichloroethane	–	45	100
	Styrene	Dichloroethane	–	22	100
	trans-β-Methylstyrene[g]	Dichloromethane	29	19	0 (ee)[h]
	cis-β-Methylstyrene[g]	Dichloromethane	73	28	2 (ee)[h]

[a] Turnover frequency calculated for 10 min of reaction.
[b] Olefin conversion at 24 h.
[c] Selectivity to the corresponding epoxides, at 24 h.
[d] Recycled catalyst.
[e] An aqueous solution (70 wt.%) of *t*-BuOOH was used.
[f] Campholenic aldehyde and epoxy campholenic aldehyde were formed with 62% and 14% selectivity, respectively.
[g] Reaction temperature = 40 °C.
[h] Enantiomeric excess (only epoxides were formed).

Considerable catalytic performance data for cyclooctene epoxidation now exists for complexes of the type $[MoO_2Cl_2L]$ (measured under similar reaction conditions) and it is clear that the equatorial donor ligands L have a strong influence. The catalytic activity of complex **2** is higher than that reported for complexes bearing 1,4-diazabutadienes (58–179 mol mol_{Mo}^{-1} h^{-1}) [29,60], 2,2′-bis[(4*S*)-4-benzyl-2-oxazoline] (147 mol mol_{Mo}^{-1} h^{-1}) [15], substituted 2,2′-bipyridines (25–248 mol mol_{Mo}^{-1} h^{-1}) [30,61] and ethylenediimines (<63 mol mol_{Mo}^{-1} h^{-1}) [62], and somewhat lower than that reported for the complex bearing ethyl[3-(2-pyridyl)-1-pyrazolyl]acetate (360 mol mol_{Mo}^{-1} h^{-1}) [63]. The catalytic activity of **1** is typical of complexes of the type $[MoO_2L]$ with tetradentate Schiff base ligands [39] and $[MoO_2(L)_2]$ with bidentate 2-pyridyl alcoholate ligands (54 mol mol_{Mo}^{-1} h^{-1}) [64].

Further tests were carried out to assess the influence of the solvent on the catalytic properties of compounds **1** and **2** for the epoxidation of cyclooctene at 55 °C. The use of aqueous *t*-BuOOH (70 wt.%) instead of the 5.5 M decane solution decreased the epoxidation rate for both catalysts, although the epoxide continued to be the only observed product (Table 3). This may be due to the insolubility of the catalysts in water and/or the coordinating ability of water towards the metal complexes, which might restrict the number of free coordination sites for the catalytic reaction. The addition of the non-coordinating co-solvents *n*-hexane or 1,2-dichloroethane (DCE) to the catalytic systems containing either compounds **1** or **2** and *t*-BuOOH in decane did not have an effect on product selectivities. However, the addition of hexane had a negative effect on the catalytic activities, most likely due to the very poor solubilities of the catalysts in this solvent. While the addition of DCE to the system containing compound **1** did not have a significant effect on the reaction rate, its addition to the system containing **2** increased the initial activity from 280 to 578 mol mol_{Mo}^{-1} h^{-1} and led to nearly quantitative epoxide yield after 10 min reaction (Fig. 3 and Table 3).

For cyclooctene epoxidation using *t*-BuOOH in decane and no additional co-solvent, the catalysts were successfully separated from the reactants and products by adding *n*-hexane to the reaction solution after a catalytic run of 24 h. The resultant solids were washed thoroughly with *n*-hexane, dried at room temperature and used in a second run. Product selectivity remained unchanged for both systems. However, from the first to the second run, epoxide yield at 24 h decreased from 98 to 88% for **2** and from 75 to 57% for **1**. FTIR and Raman spectra were measured for the solids recovered after the first run. The FTIR spectra for both of the used catalysts showed new bands at 1655 and 1705 cm^{-1} [as high frequency shoulders on the band at 1630 cm^{-1} assigned to C=N(imine) stretching], the origin of which is unclear at the time of writing. Apart from these two bands, the IR and Raman spectra of the used catalyst **1** remained essentially unchanged compared with those for the fresh catalyst. For the system containing complex **2**, the FTIR spectrum of the recovered catalyst was substantially different from that for the fresh catalyst. Changes in the Mo^{VI} first coordination sphere were indicated by shifts in the Mo=O symmetric stretching vibration from 967 to 943 cm^{-1} and the Mo–Cl stretching frequency from 336 to 352 cm^{-1}. Some changes were also noted for the bands related with the ligand oep-H_2saldpen. For example, bands in the range of 700–760 cm^{-1} changed from 704, 728, 749 and 759 cm^{-1} for the fresh catalyst, to 699 and 759 cm^{-1} for the used catalyst. The band at 728 cm^{-1} has been assigned to the C–H out-of-plane bending of pyrrole and therefore its disappearance in the spectrum for the used catalyst suggests either loss or modification of the pyrrole groups. Work is in progress to fully characterise and elucidate the natures of the used catalysts derived from **1** and **2**.

The catalytic performance of complexes **1** and **2** was further investigated in the oxidation of other olefins, namely (*R*)-(+)-limonene, styrene and α-pinene, using DCE as a co-solvent, at 55 °C. Catalytic activity is always higher for **2** than for **1**, and tends to decrease as the olefin becomes less substituted and, therefore, less reactive, following the order: *cis*-cyclooctene > (*R*)-(+)-limonene > α-pinene > styrene (Table 3). This trend is consistent with the mechanistic assumptions mentioned above, since the higher electronic density of an internal olefinic double bond (compared with a terminal C=C bond) should favour nucleophilic attack on an electrophilic oxidising species. For all substrates, complex **1** only exhibited epoxidation activity. Reactive epoxides such as styrene oxide did not undergo consecutive epoxide ring opening reactions, suggesting that **1** is a quite efficient and selective catalyst for olefin epoxidation. A similar high selectivity was observed for compound **2** apart from α-pinene epoxidation. In this case, pinene oxide was primarily formed, but eventually underwent epoxide ring opening to a certain extent giving campholenic aldehyde as a major by-product.

Since the *salen*-type ligand oep-H_2saldpen has chirality centres, the chiral induction abilities of **1** and **2** were investigated in the asymmetric epoxidation of *cis*- and *trans*-β-methylstyrene with *t*-BuOOH in decane, using dichloromethane as a co-solvent, at 40 °C. The corresponding epoxide enantiomers were the only observed products, namely (1*R*,2*R*)-(+)-1-phenylpropylene oxide and (1*S*,2*S*)-(−)-1-phenylpropylene oxide from *trans*-β-methylstyrene, and the (*S*,*R*)-(−) and (*R*,*S*)-(−) enantiomers from *cis*-β-methylstyrene. As observed for the other olefins, compound **2** is more active than **1**. The conversion of *cis*-β-methylstyrene was faster than that of the *trans* diastereoisomer, especially in the presence of **2**, suggesting that the interaction of the *cis* spatial configuration of the reacting olefin with the active oxidising species is less hindered than the *trans* one (Table 3). Less than 6 and 28% β-methylstyrene conversion was achieved after 24 h in the presence of **1** and **2**, respectively, and the enantiomeric excesses were very low or negligible. Based on these results, compounds **1** and **2** do not seem to be suitable catalysts for asymmetric epoxidations.

4. Conclusions

Two monomeric *cis*-dioxomolybdenum(VI) complexes bearing a *salen*-type ligand in either tetradentate or bidentate coordination were synthesised and tested as catalysts for olefin epoxidation. The bis(chloro) complex is the more active of

the two and compares very favourably with other complexes of the type $[MoO_2Cl_2L]$ used as catalysts for the epoxidation of cyclooctene with *tert*-butyl hydroperoxide. We have shown, however, that the good activity is limited to the first catalytic run and that the lower activity exhibited by the recycled catalyst is due to a change in its structure compared with the as-synthesised complex. This is a fairly common occurrence for these types of complexes and is driving our ongoing efforts to fully characterise the catalysts both during and after the epoxidation reactions.

Acknowledgments

The authors are grateful to FCT, OE and FEDER for funding (Project POCI/QUI/56109/2004). S.M.B. thanks the University of Aveiro for research grants. S.S.B. and C.S. are grateful to the FCT for post-doctoral grants.

Appendix A. Supplementary data

Supplementary data associated with this article can be found, in the online version, at doi:10.1016/j.molcata.2007.01.050.

References

[1] A.S. Rao, in: B.M. Trost, I. Fleming, S.V. Ley (Eds.), Comprehensive Organic Synthesis, vol. 7, Pergamon, Oxford, 1991, p. 357, and references cited therein.
[2] J.W. Schwesinger, T. Bauer, in: G. Helmchen, R.W. Hoffmann, J. Mulzer, E. Schaumann (Eds.), Stereoselective Synthesis, E21e, Houben Weyl Thieme, New York, 1995, pp. 4599–4648.
[3] K.A. Jorgensen, Chem. Rev. 89 (1989) 431.
[4] P. Chaumette, H. Mimoun, L. Saussine, J. Fischer, A. Mitschler, J. Organomet. Chem. 250 (1983) 291, and references cited therein.
[5] J.-M. Brégeault, J. Chem. Soc., Dalton Trans. (2003) 3289.
[6] J. Kollar, Halcon, US Patents 3,350,422 and 3,351,635 (1967).
[7] M.N. Sheng, G.J. Zajaczek, ARCO, GB Patent 1,136,923 (1968).
[8] W.A. Herrmann, J.J. Haider, J. Fridgen, G.M. Lobmaier, M. Spiegler, J. Organomet. Chem. 603 (2000) 69.
[9] J.M. Mitchell, N.S. Finney, J. Am. Chem. Soc. 123 (2001) 862.
[10] A.M. Santos, F.E. Kühn, K. Bruus-Jensen, I. Lucas, C.C. Romão, E. Herdtweck, J. Chem. Soc. Dalton Trans. (2001) 1332.
[11] Y.-L. Wong, D.K.P. Ng, H.K. Lee, Inorg. Chem. 41 (2002) 5276.
[12] J. Zhao, X.G. Zhou, A.M. Santos, E. Herdtweck, C.C. Romão, F.E. Kühn, J. Chem. Soc. Dalton Trans. (2003) 3736.
[13] J.A. Brito, M. Gómez, G. Muller, H. Teruel, J.-C. Clinet, E. Duñach, M.A. Maestro, Eur. J. Inorg. Chem. (2004) 4278.
[14] S. Gago, J.E. Rodríguez-Borges, C. Teixeira, A.M. Santos, J. Zhao, M. Pillinger, C.D. Nunes, Z. Petrovski, T.M. Santos, F.E. Kühn, C.C. Romão, I.S. Gonçalves, J. Mol. Catal. A: Chem. 236 (2005) 1.
[15] S.M. Bruno, B. Monteiro, M.S. Balula, F.M. Pedro, M. Abrantes, A.A. Valente, M. Pillinger, P. Ribeiro-Claro, F.E. Kühn, I.S. Gonçalves, J. Mol. Catal. A: Chem. 260 (2006) 11.
[16] E.P. Carreiro, G. Yong-En, A.J. Burke, Inorg. Chim. Acta 359 (2006) 1519.
[17] A.U. Barlan, A. Basak, H. Yamamoto, Angew. Chem. Int. Ed. 45 (2006) 5849.
[18] W.R. Thiel, J. Eppinger, Chem. Eur. J. 3 (1997) 696.
[19] W.R. Thiel, M. Angstl, T. Priermeier, Chem. Ber. 127 (1994) 2373.
[20] W.R. Thiel, M. Angstl, N. Hansen, J. Mol. Catal. A: Chem. 103 (1995) 5.
[21] W.R. Thiel, T. Priermeier, Angew. Chem. Int. Ed. Engl. 34 (1995) 1737.
[22] C. Freund, M. Abrantes, F.E. Kühn, J. Organomet. Chem. 691 (2006) 3718.
[23] H. Mimoun, I. Seree de Roch, L. Sajus, Tetrahedron 26 (1970) 37.
[24] K.B. Sharpless, J.M. Townsend, D.R. Williams, J. Am. Chem. Soc. 94 (1972) 295.
[25] I.V. Yudanov, C. Di Valentin, P. Gisdakis, N. Rösch, J. Mol. Catal. A: Chem. 158 (2000) 189.
[26] F.E. Kühn, M. Groarke, É. Bencze, E. Herdtweck, A. Prazeres, A.M. Santos, M.J. Calhorda, C.C. Romão, I.S. Gonçalves, A.D. Lopes, M. Pillinger, Chem. Eur. J. 8 (2002) 2370.
[27] M. Groarke, I.S. Gonçalves, W.A. Herrmann, F.E. Kühn, J. Organomet. Chem. 649 (2002) 108.
[28] F.E. Kühn, W.-M. Xue, A. Al-Ajlouni, A.M. Santos, S.L. Zang, C.C. Romão, G. Eickerling, E. Herdtweck, Inorg. Chem. 41 (2002) 4468.
[29] A.A. Valente, J. Moreira, A.D. Lopes, M. Pillinger, C.D. Nunes, C.C. Romão, F.E. Kühn, I.S. Gonçalves, New J. Chem. 28 (2004) 308.
[30] A. Al-Ajlouni, A.A. Valente, C.D. Nunes, M. Pillinger, A.M. Santos, J. Zhao, C.C. Romão, I.S. Gonçalves, F.E. Kühn, Eur. J. Inorg. Chem. 2005 (1716).
[31] L.F. Veiros, A. Prazeres, P.J. Costa, C.C. Romão, F.E. Kühn, M.J. Calhorda, Dalton Trans. (2006) 1383.
[32] K. Yamanouchi, S. Yamada, Inorg. Chim. Acta 9 (1974) 161.
[33] W.E. Hill, N. Atabay, C.A. McAuliffe, F.P. McCullough, S.M. Razzoki, Inorg. Chim. Acta 35 (1979) 35.
[34] M. Gullotti, A. Pasini, G.M. Zanderighi, G. Ciani, A. Sironi, J. Chem. Soc. Dalton Trans (1981) 902.
[35] H. Elias, F. Stock, C. Röhr, Acta Crystallogr. C53 (1997) 862.
[36] C. Sun, X.-Y. Wang, Z.-G. Zhang, H.-C. Shi, Chin. J. Org. Chem. 24 (2004) 547.
[37] W. Schilf, B. Kamieński, Z. Rozwadowski, K. Ambroziak, B. Bieg, T. Dziembowska, J. Mol. Struct. 700 (2004) 61.
[38] K. Ambroziak, R. Pelech, E. Milchert, T. Dziembowska, Z. Rozwadowski, J. Mol. Catal. A: Chem. 211 (2004) 9.
[39] X. Zhou, J. Zhao, A.M. Santos, F.E. Kühn, Z. Naturforsch 59b (2004) 1223.
[40] M. Andrade, C. Sousa, J.E. Borges, C. Freire, J. Phys. Org. Chem. 18 (2005) 935.
[41] T. Kottke, D. Stalke, J. Appl. Crystallogr. 26 (1993) 615.
[42] R. Hooft, Collect: Data Collection Software, Delft, The Netherlands, Nonius B.V., 1998.
[43] Z. Otwinowski, W. Minor, in: C.W. Carter Jr., R.M. Sweet (Eds.), Methods in Enzymology, vol. 276, Academic Press, New York, 1997, p. 307.
[44] R.H. Blessing, Acta Cryst. A 51 (1995) 33.
[45] R.H. Blessing, J. Appl. Crystallogr. 30 (1997) 421.
[46] G.M. Sheldrick, SHELXS-97, Program for Crystal Structure Solution, University of Göttingen, 1997.
[47] G.M. Sheldrick, SHELXL-97, Program for Crystal Structure Refinement, University of Göttingen, 1997.
[48] M.J. Frisch, G.W. Trucks, H.B. Schlegel, G.E. Scuseria, M.A. Robb, J.R. Cheeseman, J.A. Montgomery, Jr., T. Vreven, K.N. Kudin, J.C. Burant, J.M. Millam, S.S. Iyengar, J. Tomasi, V. Barone, B. Mennucci, M. Cossi, G. Scalmani, N. Rega, G.A. Petersson, H. Nakatsuji, M. Hada, M. Ehara, K. Toyota, R. Fukuda, J. Hasegawa, M. Ishida, T. Nakajima, Y. Honda, O. Kitao, H. Nakai, M. Klene, X. Li, J.E. Knox, H.P. Hratchian, J.B. Cross, C. Adamo, J. Jaramillo, R. Gomperts, R.E. Stratmann, O. Yazyev, A.J. Austin, R. Cammi, C. Pomelli, J.W. Ochterski, P.Y. Ayala, K. Morokuma, G.A. Voth, P. Salvador, J.J. Dannenberg, V.G. Zakrzewski, S. Dapprich, A.D. Daniels, M.C. Strain, O. Farkas, D.K. Malick, A.D. Rabuck, K. Raghavachari, J.B. Foresman, J.V. Ortiz, Q. Cui, A.G. Baboul, S. Clifford, J. Cioslowski, B.B. Stefanov, G. Liu, A. Liashenko, P. Piskorz, I. Komaromi, R.L. Martin, D.J. Fox, T. Keith, M.A. Al-Laham, C.Y. Peng, A. Nanayakkara, M. Challacombe, P.M.W. Gill, B. Johnson, W. Chen, M.W. Wong, C. Gonzalez, and J.A. Pople, Gaussian 03, Revision A.1, Gaussian Inc., Pittsburgh, PA, 2003.
[49] T.H. Dunning Jr., P.J. Hay, in: H.F. Schaefer (Ed.), Modern Theoretical Chemistry, vol. 3, Plenum, New York, 1976, pp. 1–28.
[50] R.D. Johnson III (Ed.), NIST Computational Chemistry Comparison and Benchmark Database, NIST Standard Reference Database Number 101, Release 12, Aug 2005, http://srdata.nist.gov/cccbdb.
[51] N.B. Pahor, M. Calligaris, G. Nardin, L. Randaccio, Acta Cryst. B 34 (1978) 1360.
[52] J. Bernstein, R.E. Davis, L. Shimoni, N.L. Chang, Angew. Chem. Int. Ed. Engl. 34 (1995) 1555.
[53] J. Liimatainen, A. Lehtonen, R. Sillanpää, Polyhedron 19 (2000) 1133.
[54] L.S. Gonzales, K.S. Nagaraja, Polyhedron 6 (1987) 1635.

[55] S.M. Bruno, C.C.L. Pereira, M.S. Balula, M. Nolasco, A.A. Valente, A. Hazell, M. Pillinger, P. Ribeiro-Claro, I.S. Gonçalves, J. Mol. Catal. A: Chem. 261 (2006) 79.

[56] In a further attempt to investigate the solid state structure for compound **2**, the ^{13}C CP MAS NMR spectrum was recorded. Due to overlap between several relatively broad peaks, it was not possible to make any conclusions about the type(s) of isomer(s) present. Tentative assignments: $\delta = 171.4$ (*C*═O), 157.8 (N═*C*H), 152.8 (*C*2-OH), 139.0, 137.2 (*C*3-OCO and arom *C*b), 131.5 (arom *C*), 120.6 (*C*αα′-pyrrole and arom *C*), 109.1 (*C*ββ′-pyrrole), 60.1 (*C*a), 42.5 (*C*2′H_2), 36.3 (*C*1′H_2) ppm.

[57] R.A. Sheldon, J.K. Kochi, Adv. Catal. 25 (1976) 272.

[58] G. Wahl, D. Kleinhenz, A. Schorm, J. Sundermeyer, R. Stowasser, C. Rummey, G. Bringmann, C. Fickert, W. Kiefer, Chem. Eur. J. 5 (1999) 3237.

[59] C. Fickert, V. Nagel, W. Kiefer, G. Wahl, J. Sundermeyer, J. Mol. Struct. 482–483 (1999) 59.

[60] C.D. Nunes, M. Pillinger, A.A. Valente, A.D. Lopes, I.S. Gonçalves, Inorg. Chem. Commun. 6 (2003) 1228.

[61] C.D. Nunes, A.A. Valente, M. Pillinger, A.C. Fernandes, C.C. Romão, J. Rocha, I.S. Gonçalves, J. Mater. Chem. 12 (2002) 1735.

[62] Z. Petrovski, M. Pillinger, A.A. Valente, I.S. Gonçalves, A. Hazell, C.C. Romão, J. Mol. Catal. A: Chem. 227 (2005) 67.

[63] S.M. Bruno, J.A. Fernandes, L.S. Martins, I.S. Gonçalves, M. Pillinger, P. Ribeiro-Claro, J. Rocha, A.A. Valente, Catal. Today 114 (2006) 263.

[64] A.A. Valente, I.S. Gonçalves, A.D. Lopes, J.E. Rodríguez-Borges, M. Pillinger, C.C. Romão, J. Rocha, X. García-Mera, New J. Chem. 25 (2001) 959.